

Possibilistic Fuzzy Local Information C-Means for Sonar Image Segmentation

Alina Zare, Nicholas Young, Daniel Suen
 Electrical and Computer Engineering
 University of Florida
 Gainesville, FL 32611
 {azare, ndy14, dsuen1}@ufl.edu

Thomas Nabelek, Aquila Galusha, James Keller
 Computer Science and Electrical Engineering
 University of Missouri
 Columbia, MO 65211
 kellerj@missouri.edu

Abstract—Side-look synthetic aperture sonar (SAS) can produce very high quality images of the sea-floor. When viewing this imagery, a human observer can often easily identify various sea-floor textures such as sand ripple, hard-packed sand, sea grass and rock. In this paper, we present the Possibilistic Fuzzy Local Information C-Means (PFLICM) approach to segment SAS imagery into sea-floor regions that exhibit these various natural textures. The proposed PFLICM method incorporates fuzzy and possibilistic clustering methods and leverages (local) spatial information to perform soft segmentation. Results are shown on several SAS scenes and compared to alternative segmentation approaches.

I. INTRODUCTION

High-resolution Synthetic Aperture SONAR (SAS) systems have the image resolution and detail needed to be able to distinguish between different sea-floor environmental contexts such as sand ripple, hard-packed sand and sea grass. These systems also have the resolution and detail needed for automated target object detection and classification. However, underwater target objects may display varying characteristics across environmental contexts. For example, target signatures may be hidden or masked to varying degrees depending on the sea-floor type in which they are found. Therefore, methods that can identify the seabed environment can be used to within an automated scene understanding system or to assist in target classification and detection in an environmentally adaptive or context-dependent approach. Furthermore, the boundaries between sea-floor types are often gradual with wide regions of transition [1]. Thus, a soft segmentation approach that can identify and characterize these gradual transition regions are necessary.

In this paper, we present a soft segmentation algorithm that leverages local spatial information to encourage smooth segmentation maps and estimates both possibilistic typicality and fuzzy membership values to identify outliers and to discriminate between the various sea-floor types.

II. PROPOSED METHOD: PFLICM

Our proposed PFLICM algorithm merges previous approaches for possibilistic fuzzy clustering and soft segmentation of imagery. Namely, PFLICM combines the Possibilistic-Fuzzy Clustering algorithm, PFCLM [2], and the Fuzzy Local Information C-Means, FLICM, algorithm [3]. These ap-

proaches are blended by PFLICM through the objective function shown in (1):

$$\begin{aligned} J = & \sum_{c=1}^C \sum_{n=1}^N a u_{cn}^m \left(\| \mathbf{x}_n - \mathbf{c}_c \|_2^2 + G_{cn} \right) \\ & + b t_{cn}^q \| \mathbf{x}_n - \mathbf{c}_c \|_2^2 + \sum_{c=1}^C \gamma_c \sum_{n=1}^N (1 - t_{cn})^q \end{aligned} \quad (1)$$

such that

$$u_{cn} \geq 0 \quad \forall n = 1, \dots, N; \quad \sum_{c=1}^C u_{cn} = 1 \quad (2)$$

where \mathbf{x}_n is a $d \times 1$ column vector representing the n^{th} pixel, C is the number of clusters being estimated, \mathbf{c}_c is a $d \times 1$ vector of c^{th} cluster center, weight u_{cn} is the membership value of the n^{th} pixel in the c^{th} cluster, t_{cn} is the typicality value of the n^{th} pixel in the c^{th} cluster, a, b , and α are fixed parameter values used to balance the terms of the objective function, and m and q are fixed “fuzzifier” parameters which control the degree of sharing across the clusters and the degree to which points may be labeled as outliers, respectively. Also,

$$G_{cn} = \sum_{\substack{k \in \mathcal{N}_n \\ k \neq n}} \frac{1}{d_{nk} + 1} (1 - u_{ck})^m \| \mathbf{x}_k - \mathbf{c}_c \|_2^2, \quad (3)$$

where \mathbf{x}_n is the center pixel in the local window under consideration, \mathcal{N}_n is the neighborhood around the center pixel (i.e., a neighborhood defined by fixed radius), d_{nk} is the Euclidean distance between the image indices between \mathbf{x}_n and \mathbf{x}_k . These terms are further defined and explained in the following subsections.

1) *Soft Segmentation with Local Information*: The first term in (1), $\sum_{c=1}^C \sum_{n=1}^N a u_{cn}^m \left(\| \mathbf{x}_n - \mathbf{c}_c \|_2^2 + G_{cn} \right)$, follows directly from the objective function of the FLICM algorithm [3]. This term combines fuzzy clustering [4] (and the estimation of fuzzy membership values) with local spatial information to encourage neighboring pixels to have similar fuzzy membership values. In particular, during minimization of (1), larger fuzzy membership values, u_{cn} , for a data point n will be assigned to clusters in which the both the distance between the data point and the cluster center is relatively small ($\| \mathbf{x}_n - \mathbf{c}_c \|_2^2$) and where the G_{cn} value is small. The

G_{cn} term can be interpreted as a penalty for clusters in which neighboring pixels have a small membership value.

2) *Outlier Identification with Possibilistic Clustering*: The inclusion of the $bt_{cn}^q \|\mathbf{x}_n - \mathbf{c}_c\|_2^2$ and $\gamma_c(1 - t_{cn})^q$ terms provide for the identification of outliers in the input SAS imagery. These terms are adapted from the Possibilistic clustering [5] and Possibilistic-Fuzzy clustering algorithms [2]. Possibilistic clustering methods estimate the *typicality*, t_{cn} , of each data point and, unlike the membership values, u_{cn} , are not constrained to sum-to-one across clusters. When the typicality of a data point is close to zero for a particular cluster, that indicates that the data point is an outlier with respect to that cluster. A data point that is an outlier in all clusters (i.e., sufficiently far from all cluster centers) will have a low typicality value in all clusters. Thus, the estimated typicality values identify the outliers in an input data set and prevent them from influencing cluster estimation and biasing the resulting cluster representative values. This is an important feature for locating noise pixels as well as for excluding anomalous (e.g., target object) pixels while characterizing the background and sea-floor. In this way, potential target objects in a scene do not affect the sea-floor segmentation results.

3) *Alternating Optimization Approach*: Cluster centers, membership, and typicality values are estimated using alternating optimization. All values are initialized and, then, the parameters are updated iteratively. Solving $\frac{\partial J}{\partial \mathbf{c}_c} = 0$ results in the following update equation for the endmembers,

$$\mathbf{c}_c = \frac{\sum_n (au_{cn}^r + bt_{cn}^q) \mathbf{x}_n}{\sum_n (au_{cn}^r + bt_{cn}^q)} \quad (4)$$

The update equation for the membership values is found by adding a Lagrange multiplier term to enforce the sum-to-one constraint on the membership values, resulting in:

$$u_{cn} = \frac{1}{\sum_{k=1}^C \left(\frac{(\mathbf{x}_n - \mathbf{c}_c)(\mathbf{x}_n - \mathbf{c}_c)^T + G_{cn}}{(\mathbf{x}_n - \mathbf{c}_k)(\mathbf{x}_n - \mathbf{c}_k)^T + G_{kn}} \right)^{\frac{1}{r-1}}} \quad (5)$$

The update equation for the typicalities value is found to be:

$$t_{cn} = \frac{1}{1 + \left(\frac{b}{\gamma_c} \|\mathbf{x}_n - \mathbf{c}_c\|_2^2 \right)^{\frac{1}{q-1}}} \quad (6)$$

where the γ_c value is set to be the mean of the $\|\mathbf{x}_n - \mathbf{c}_c\|_2^2$ value for all of the pixels in the associated cluster. Therefore, each iteration, the γ_i value gets updated.

Given these update equations, the proposed PFLICM algorithm is summarized below.

Algorithm 1 PFLICM

Initialize membership values to $\frac{1}{C}$, typicality values to 1, and randomly select input data points as the C initial cluster centers.

REPEAT

 Update cluster centers $\{\mathbf{c}_c\}_{c=1,\dots,C}$ using (4)

 Update the memberships using (5)

 Update the typicalities using (6)

UNTIL convergence

III. APPLICATION TO SAS IMAGERY

Our application of PFLICM to SAS imagery for sea-floor segmentation is comprised of three major components: (1) feature extraction, (2) superpixel segmentation, and (3) application of PFLICM. The first component, feature extraction, is carried out in order to produce segmentation results that fall along the boundaries of the distinct sea-floor textures. The features extracted were selected to highlight the differences between textures of interest. The features used were a Sobel edge histogram descriptor [6], histogram of oriented gradients [7], and local binary pattern features [8]. The Sobel edge histogram descriptor was generated by applying the Sobel edge detector for vertical, diagonal, horizontal and anti-diagonal edges. Then, each pixel is labeled with the edge type that returned the largest Sobel edge detection value or it is marked as “no edge” if all of the detection values were below a prescribed threshold of 0.5. Then, the feature vector associated with each pixel is the histogram of edge types for the surrounding 17×17 -size neighborhood. The HOG features were generated using cell and block sizes of 2×2 , a 1 pixel block overlap, 9 bins, computed over a sliding window size of 5×5 . Finally, the LBP features were generated using 3×3 sized cells.

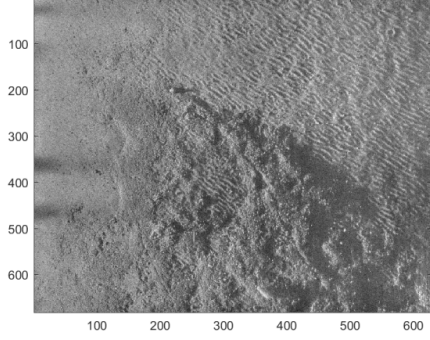
As opposed to applying PFLICM to every individual pixel in a SAS image, in our implementation input grayscale SAS imagery are first oversegmented using the SLIC superpixel segmentation algorithm [9]. Then, the feature vectors associated with each resulting superpixel are averaged and center location of the superpixel is marked as the location (i.e., the image row and column) to which this average feature vector corresponds. Then, PFLICM is applied to only these feature vectors that summarize each superpixel. The use of superpixels (instead of individual pixels from the input image) significantly reduces the overall computation required. Figure 1 shows an example input image and its resulting superpixel segmentation.

After feature extraction and superpixel segmentation, the PFLICM algorithm is applied to the set of average feature vectors associated with each superpixel. After applying PFLICM, the resulting segmentation can be examined by creating the *product maps* which are generated by computing the product of the estimated membership and typicality value for each superpixel and, then, assigning this value to each individual pixel associated with that superpixel. Specifically, the value of a product map, \mathbf{P} at pixel n for cluster c is computed as $\mathbf{P}_c(n) = u_{cn} t_{cn}$.

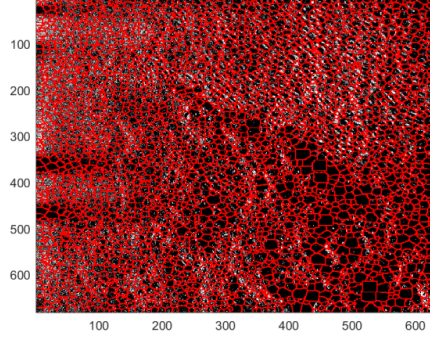
IV. EXPERIMENTAL RESULTS

In the first set of results PFLICM was applied to seven images with the following parameter settings:

- Membership weight $a = 14$
- Typicality weight $b = 0.3$
- Fuzzifier for Fuzzy Clustering Term $m = 1.8$
- Fuzzifier for Possibilistic Clustering Term $q = 2.2$
- Change threshold (stopping criteria) $\epsilon = 1e-6$
- Number of clusters = 3



(a) Original SAS Image



(b) Superpixel Segmentation of SAS Image

Fig. 1. (a) Original SAS image shows a variety of textures including “flat sand,” “sand ripple,” and “rock.” (b) Superpixel segmentation of the image into 3500 superpixels.

- Radius of neighborhood window $\mathcal{N}_n = \infty$ (All superpixels in the image were considered to be in the same neighborhood.)

The parameters were determined manually. For comparison, each image was also segmented using the FLICM algorithm and the PFCM algorithm (using the same parameter settings as applied for PFLICM for the associated parameters across the algorithms). Unless otherwise noted, each set of images displays the most relevant values - that is, the product maps are shown for PFLICM and PFCM while the membership maps are shown for FLICM (since FLICM does not generate typicality values).

The results of the seven images are shown in Figs. 3 and 6 through 11.

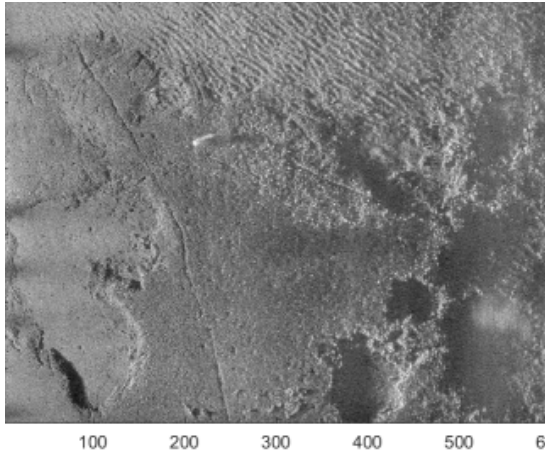
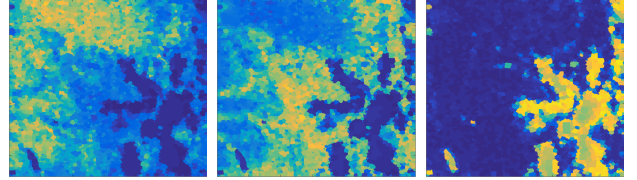
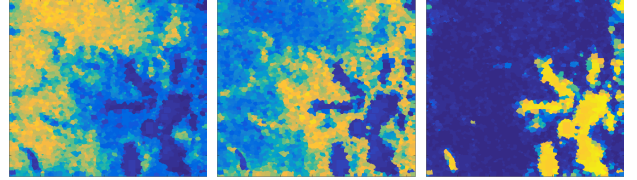


Fig. 2. SAS image containing sand ripples, flat sand with large holes, and an outlier.

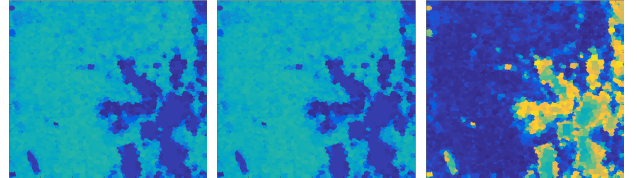
Since PFLICM estimates typicality in addition to membership, it is able to disregard potential outliers. Figure 4 shows the typicality maps of PFLICM and PFCM and the membership map of FLICM. Note that the typicality maps of PFLICM and PFCM are identical because the fuzzy factor G_{cn} does not



(a) PFLICM Cluster 1 (b) PFLICM Cluster 2 (c) PFLICM Cluster 3



(d) FLICM Cluster 1 (e) FLICM Cluster 2 (f) FLICM Cluster 3



(g) PFCM Cluster 1 (h) PFCM Cluster 2 (i) PFCM Cluster 3

Fig. 3. Clustering results of Fig. 2 given by the PFLICM (a-c), FLICM (d-f), and PFCM (g-i) algorithms. Clusters have been manually aligned for easy comparison.

contribute to typicality. Figure 5 provides zoomed in images on the typicality and membership maps of Figure 4 (Typicality maps only shown once to avoid redundancy because of the aforementioned equality). Notice how the typicality maps (b-d) clearly diminish the value at the outlier, while the membership maps (e-g) do not. Thus, PFLICM maintains the ability of PFCM to identify and effectively nullify the contribution of outliers.

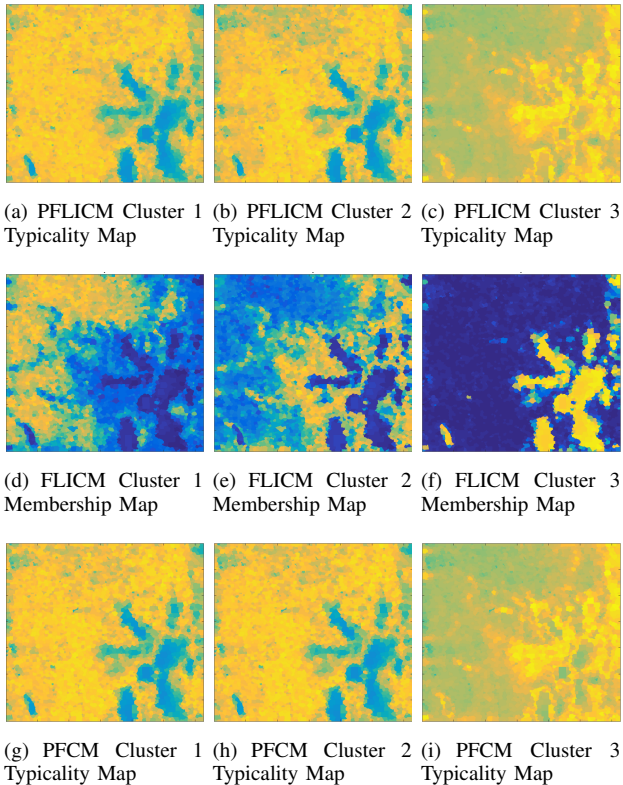
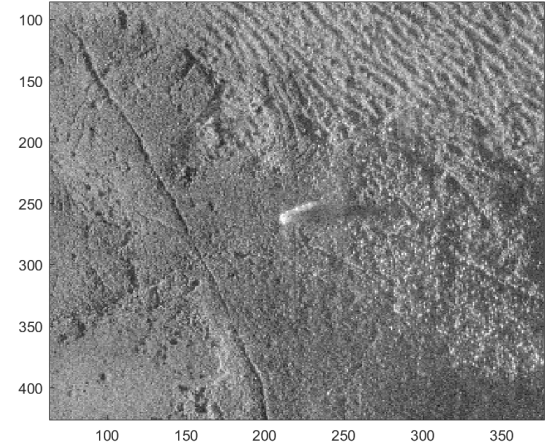


Fig. 4. Clustering results on image (a) from Figure 3 displaying the typicalities of PFLICM (a-c), memberships of FLICM (d-f), and typicalities of PFCM (g-i).



(a) Sub-Image containing an outlier object

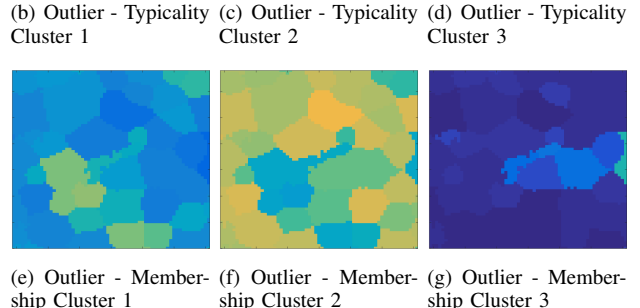
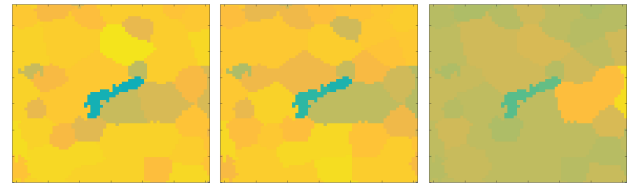
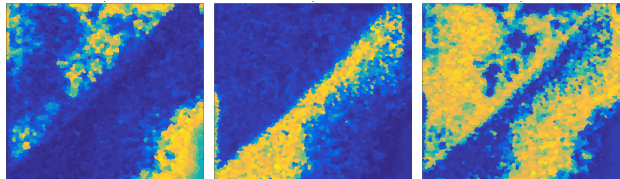


Fig. 5. (a) Sub-Image containing an outlier obtained from the image (in Fig. 2. (b-d) show a zoomed in area around the outlier of the typicality maps from Figure 4 centered on the outlier. (e-g) show a zoomed in area around the outlier on the membership maps from Figure 4 centered on the outlier.

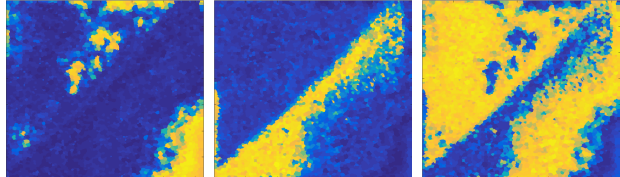
Figures 5 - 10 provide additional evidence of the utility of this spatial fuzzy and possibilistic approach to seafloor segmentation. These results illustrate how PFLICM blends the strengths of both FLICM and PFCM into a single set of results. Namely, the PFLICM algorithm maintains the membership smoothness and encourages sparse membership values when appropriate (as found with FLICM) while still mitigating the effects of outliers (an attribute characteristic of PFCM).



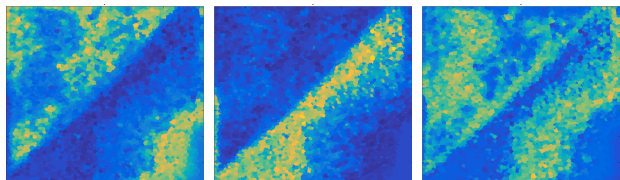
(a) Original Image



(b) PFLICM Cluster 1 (c) PFLICM Cluster 2 (d) PFLICM Cluster 3

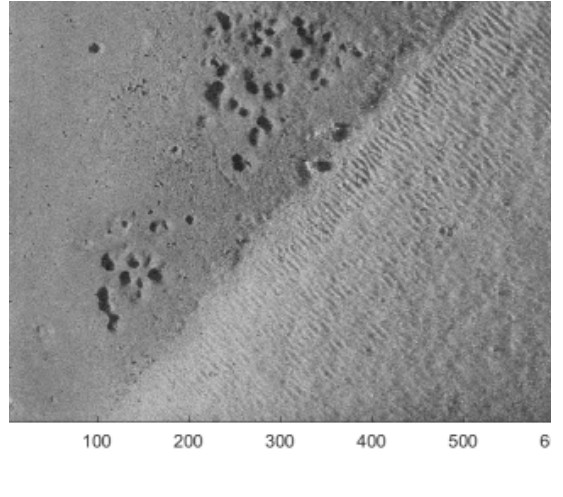


(e) FLICM Cluster 1 (f) FLICM Cluster 2 (g) FLICM Cluster 3

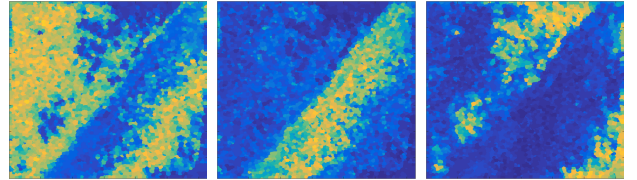


(h) PFCM Cluster 1 (i) PFCM Cluster 2 (j) PFCM Cluster 3

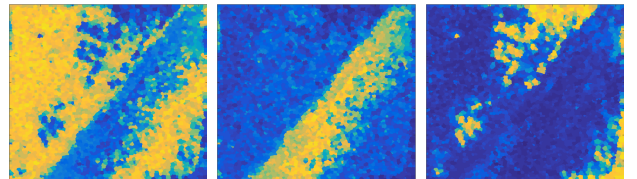
Fig. 6. (a) Image containing sand ripples, hard-packed sand, and holes. Clustering results of image (a) given by the PFLICM (b-d), FLICM (e-g), and PFCM (h-j) algorithms. Clusters have been manually aligned for easy comparison.



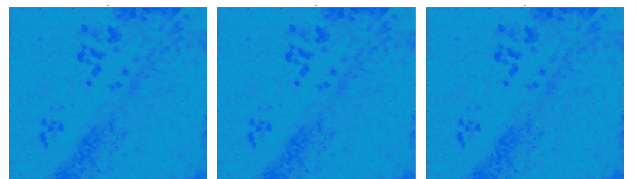
(a) Original Image



(b) PFLICM Cluster 1 (c) PFLICM Cluster 2 (d) PFLICM Cluster 3

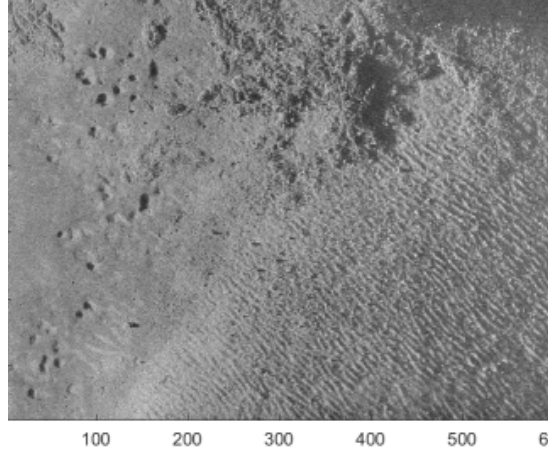


(e) FLICM Cluster 1 (f) FLICM Cluster 2 (g) FLICM Cluster 3

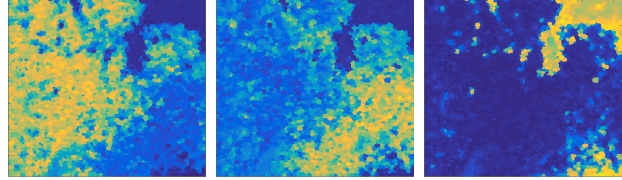


(h) PFCM Cluster 1 (i) PFCM Cluster 2 (j) PFCM Cluster 3

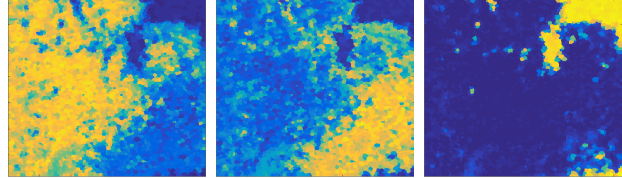
Fig. 7. (a) Image containing sand ripples, hard-packed sand, and holes. Clustering results of image (a) given by the PFLICM (b-d), FLICM (e-g), and PFCM (h-j) algorithms. Clusters have been manually aligned for easy comparison.



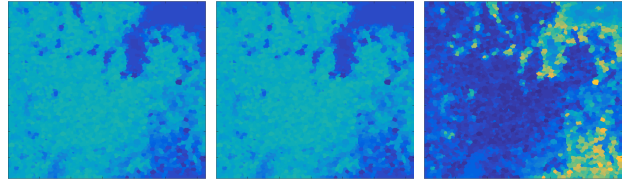
(a) Original Image



(b) PFLICM Cluster 1 (c) PFLICM Cluster 2 (d) PFLICM Cluster 3

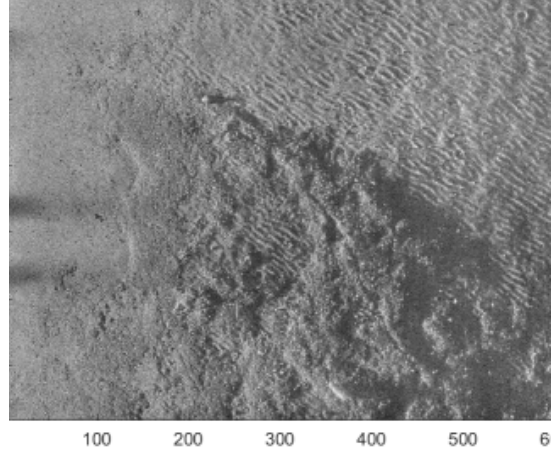


(e) FLICM Cluster 1 (f) FLICM Cluster 2 (g) FLICM Cluster 3

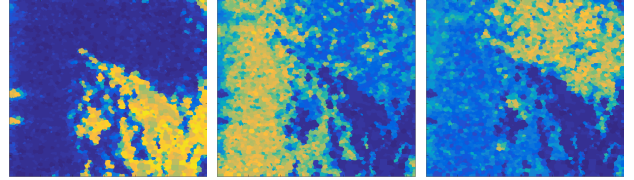


(h) PFCM Cluster 1 (i) PFCM Cluster 2 (j) PFCM Cluster 3

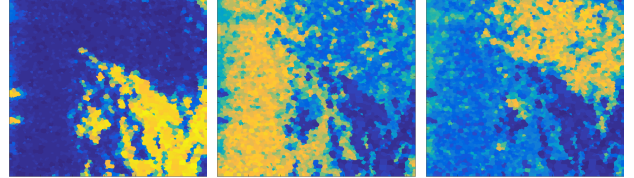
Fig. 8. (a) Image containing sand ripples, smooth sand, and hilly regions with shadows. Clustering results of image (a) given by the PFLICM (b-d), FLICM (e-g), and PFCM (h-j) algorithms. Clusters have been manually aligned for easy comparison.



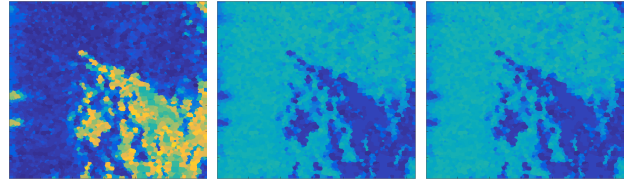
(a) Original Image



(b) PFLICM Cluster 1 (c) PFLICM Cluster 2 (d) PFLICM Cluster 3

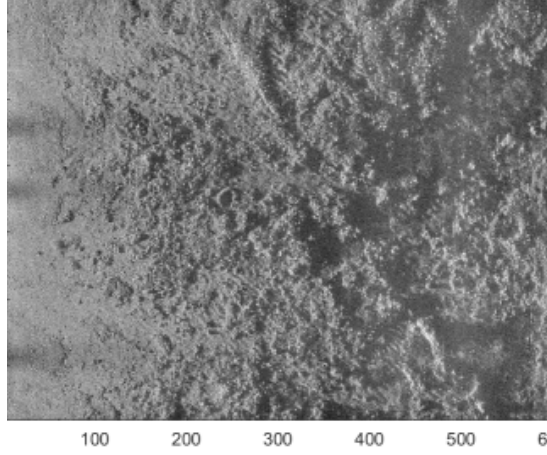


(e) FLICM Cluster 1 (f) FLICM Cluster 2 (g) FLICM Cluster 3



(h) PFCM Cluster 1 (i) PFCM Cluster 2 (j) PFCM Cluster 3

Fig. 9. (a) Image containing sand ripples, smooth sand, sand with hilly regions and shadows. Clustering results of image (a) given by the PFLICM (b-d), FLICM (e-g), and PFCM (h-j) algorithms. Clusters have been manually aligned for easy comparison.



100 200 300 400 500 6

(a) Original Image

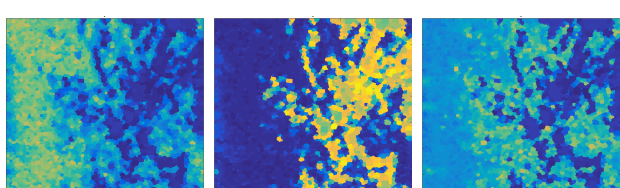
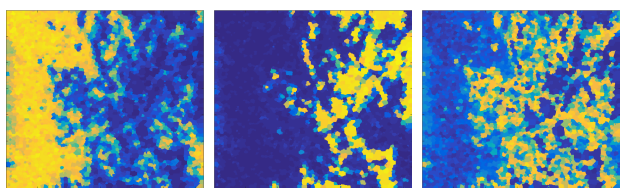
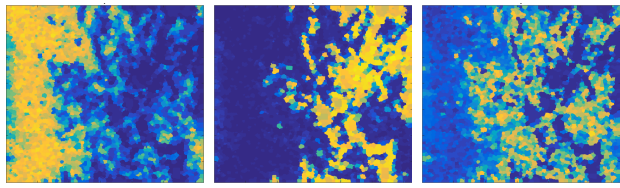
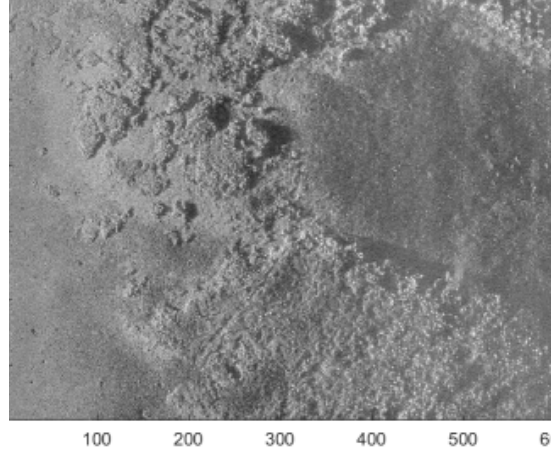


Fig. 10. (a) Image containing smooth sand and a great variety of hilly regions with shadows. Clustering results of image (a) given by the PFLICM (b-d), FLICM (e-g), and PFCM (h-j) algorithms. Clusters have been manually aligned for easy comparison.



100 200 300 400 500 6

(a) Original Image

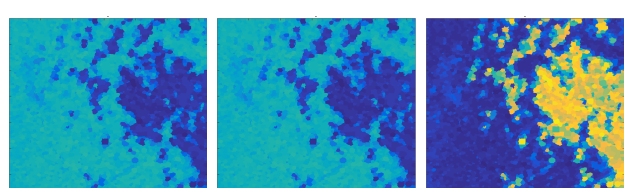
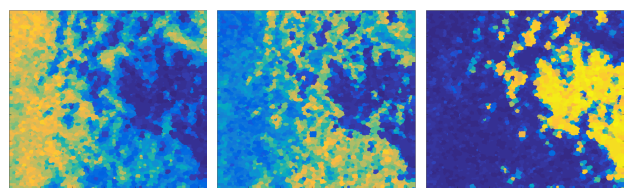
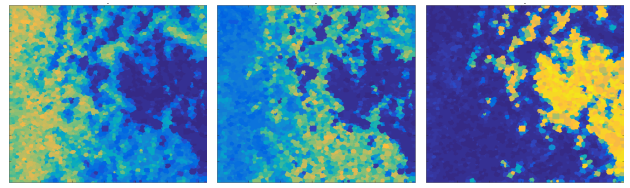


Fig. 11. (a) Image containing smooth sand, hard-packed sand, and hilly regions with shadows. Clustering results of image (a) given by the PFLICM (b-d), FLICM (e-g), and PFCM (h-j) algorithms. Clusters have been manually aligned for easy comparison.

V. SUMMARY

The possibilistic fuzzy local information c-means clustering algorithm is developed and presented with application to SAS image segmentation. PFLICM is shown to combine the advantages of multiple alternative segmentation approaches. Results show improvement over existing soft segmentation approaches and successfully identify various sea floor textures comparable to the ability of a human observer.

ACKNOWLEDGMENT

This research was funded by the Office of Naval Research Code 321.

REFERENCES

- [1] J. T. Cobb and A. Zare, "Superpixel formation and boundary detection in synthetic aperture sonar imagery," in *3rd Int. Conf. SAS and SAR*, 2014.
- [2] N. R. Pal, K. Pal, J. M. Keller, and J. C. Bezdek, "A possibilistic fuzzy c-means clustering algorithm," *IEEE Transactions on Fuzzy Systems*, vol. 13, no. 4, pp. 517–530, Aug 2005.
- [3] S. Krinidis and V. Chatzis, "A robust fuzzy local information c-means clustering algorithm," *IEEE Transactions on Image Processing*, vol. 19, no. 5, pp. 1328–1337, May 2010.
- [4] J. C. Bezdek, R. Ehrlich, and W. Full, "Fcm: The fuzzy c-means clustering algorithm," *Computers & Geosciences*, vol. 10, no. 2-3, pp. 191–203, 1984.
- [5] R. Krishnapuram and J. Keller, "A possibilistic approach to clustering," *IEEE Trans. Fuzzy Syst.*, vol. 1, no. 2, pp. 98–110, 1993.
- [6] H. Frigui and P. Gader, "Detection and discrimination of land mines in ground-penetrating radar based on edge histogram descriptors and a possibilistic k-nearest neighbor classifier," *IEEE Transactions on Fuzzy Systems*, vol. 17, no. 1, pp. 185–199, 2009.
- [7] N. Dalal and B. Triggs, "Histograms of oriented gradients for human detection," in *Computer Vision and Pattern Recognition, 2005. CVPR 2005. IEEE Computer Society Conference on*, vol. 1. IEEE, 2005, pp. 886–893.
- [8] Z. Guo, L. Zhang, and D. Zhang, "A completed modeling of local binary pattern operator for texture classification," *IEEE Transactions on Image Processing*, vol. 19, no. 6, pp. 1657–1663, 2010.
- [9] R. Achanta, A. Shaji, K. Smith, A. Lucchi, P. Fua, and S. Süsstrunk, "Slic superpixels compared to state-of-the-art superpixel methods," *IEEE transactions on pattern analysis and machine intelligence*, vol. 34, no. 11, pp. 2274–2282, 2012.